doi:10.1093/mnras/stx1130

MNRAS **469**, 4258–4267 (2017) Advance Access publication 2017 May 10

On the orbital evolution of supermassive black hole binaries with circumbinary accretion discs

Yike Tang, ^{1★} Andrew MacFadyen ^{1★} and Zoltán Haiman ^{1,2★}

¹Center for Cosmology and Particle Physics, New York University, New York, NY 10003, USA

Accepted 2017 May 8. Received 2017 May 8; in original form 2017 March 10

ABSTRACT

Gaseous circumbinary accretion discs provide a promising mechanism to facilitate the mergers of supermassive black holes (SMBHs) in galactic nuclei. We measure the torques exerted on accreting SMBH binaries, using 2D, isothermal, moving-mesh, viscous hydrodynamical simulations of circumbinary accretion discs. Our computational domain includes the entire inner region of the circumbinary disc, with the individual black holes (BHs) treated as point masses on the grid. A sink prescription is used to account for accretion on to each BH through well-resolved minidiscs. We explore a range of mass-removal rates for the sinks. We find that the torque exerted on the binary is primarily gravitational, and dominated by the gas orbiting close behind and ahead of the individual BHs. The torques are sensitive to the sink prescription: slower sinks result in more gas accumulating near the BHs and more negative torques, driving more rapid binary merger. For faster sinks, the torques are less negative, and eventually turn positive (for unphysically fast sinks). When the minidiscs are modelled as standard α discs, our results are insensitive to the chosen sink radius. When scaled to $\dot{M}/\dot{M}_{\rm Edd} = 0.3$, the implied residence time-scale is $\approx 3 \times 10^6$ yr, independent of the SMBH masses and orbital separation. For binaries with total mass $\lesssim 10^7 \, \mathrm{M_{\odot}}$, this is shorter than the inspiral time due to gravitational wave (GW) emission alone, implying that gas discs will have a significant impact on the SMBH binary population and can affect the GW signal for pulsar timing arrays.

Key words: accretion, accretion discs – black hole physics – hydrodynamics.

1 INTRODUCTION

Binaries embedded in gas discs occur frequently in nature. Examples include planet+star systems with protoplanetary discs (e.g. Ward 1997), young stellar binaries (e.g. Orosz et al. 2012) and supermassive black hole binaries (SMBHBs) expected in many galactic nuclei (e.g. Dotti, Sesana & Decarli 2012; Mayer 2013). The nature of the binary–disc interaction is of compelling interest for understanding the long-term evolution of these systems. In the case of SMBHBs, in particular, a long-standing question is whether such binaries can reach orbital separations as small as \sim 1 pc, so that gravitational radiation would cause an inevitable merger (e.g. Begelman, Blandford & Rees 1980). Gas discs could help facilitate orbital decay down to these separations (e.g. Escala et al. 2005). Understanding the interaction between SMBHBs and their gas discs is also crucial for predicting the electromagnetic signatures of such systems (e.g. Tanaka, Menou & Haiman 2012).

Significant work has been done to understand the linear binary—disc interaction in the limit of small mass ratio, $q \equiv M_2/M_1 \ll$

*E-mail: yt611@nyu.edu (YT); macfadyen@nyu.edu (AMF); zoltan@astro.columbia.edu (ZH)

1. This so-called Type I planetary migration is facilitated by linear spiral density waves launched at resonant disc locations (e.g. Goldreich & Tremaine 1980). The rate and even the direction (inwards or outwards) of Type I migration is sensitive to thermodynamics (e.g. Paardekooper & Mellema 2006). The regime $10^{-4} \lesssim q \lesssim 0.05$ has also been widely explored. The secondary opens a narrow annular gap in the disc, resulting in so-called Type II migration (e.g. Ward 1997). The interaction is non-linear, generally causing inward migration on a time-scale comparable to the viscous time-scale of the disc near the binary (e.g. Lin & Papaloizou 1986). Deviations from this time-scale can, however, be significant, especially when the mass of the smaller black hole (BH) exceeds that of the nearby disc (e.g. Syer & Clarke 1995; Ivanov, Papaloizou & Polnarev 1999; Duffell et al. 2014; Dürmann & Kley 2017).

By comparison, relatively little analogous work has been done for SMBH binaries in the range $0.1 \lesssim q \leq 1$. Studies of the demography and assembly of SMBHs in hierarchical cosmologies, based on the merger histories of dark matter haloes, find broad distributions between $10^{-2} \lesssim q < 1$, generally peaking in the range $q \sim 0.1$ –1 (e.g. Volonteri, Haardt & Madau 2003; Sesana et al. 2005; Lippai, Frei & Haiman 2009; Sesana et al. 2012). MacFadyen & Milosavljević (2008), D'Orazio, Haiman & MacFadyen (2013) and Miranda, Muñoz & Lai (2017) have made use of 2D grid-based

²Department of Astronomy, Columbia University, New York, NY 10027, USA

hydrodynamical simulations to study SMBHBs embedded in thin α discs (Shakura & Sunyaev 1973), and included a discussion of the disc torques. However, these simulations excised the innermost region surrounding the binary, and imposed an inner boundary condition, neglecting potentially important gas dynamics, and torque contributions from inside the excised region. Farris et al. (2014) included the innermost region in their simulated domain, but their study did not focus on the binary–disc interaction, and did not present measurements of the gas torques from that region. Closest to this paper are the previous studies by Cuadra et al. (2009) and Roedig et al. (2012), both of which followed the interaction between SMBHBs with q=1/3 and a self-gravitating circumbinary disc, using 3D smoothed particle hydrodynamics (SPH) simulation. We will present a comparison to these studies below.

In this work, we use a 2D grid-based code to evolve a thin (aspect ratio h/r=0.1) α disc for a few viscous times, until the system has relaxed to a quasi-steady state. We use DISCO, a high-resolution, finite-volume moving-mesh code (Duffell & MacFadyen 2011, 2012, 2013), which allows us to not impose an inner boundary condition, and therefore to include the BHs in the computational domain. Our main goal is to accurately measure the disc—binary torques, including contributions from gravitational torques, as well as effective torques from the accretion of mass and angular momentum by the BHs. Accretion is implemented with a sink prescription; we perform numerical experiments to study how the mass-removal rate in the sinks affects the global structure of the circumbinary disc and the torques exerted on the binary.

This paper is organized as follows. In Section 2, we summarize our numerical methods. In Section 3, we present our main results on the disc torques. We also determine the dependence of the disc morphology and the disc torque on the sink time-scale $\tau_{\rm sink}$. In Section 4, we discuss the implications of our results, list some caveats, and outline topics for future work. Finally, in Section 5, we summarize our conclusions. Throughout this paper, we adopt units in which Newton's constant, the binary mass and the binary separation are $G = M_{\rm bin} = 2 \times M_{\rm bh} = a = 1$, and the binary's orbital period is $t_{\rm bin} = 2\pi$.

2 NUMERICAL SETUP

2.1 Summary of simulation setup

The model and numerical setup of this work closely resembles that in our previous work (Farris et al. 2014, 2015). We only briefly outline the key aspects and some modifications here, and refer the reader to the above papers for further details. All simulations are performed using the DISCO code in 2D; a recent version of this code, including 3D magnetohydrodynamics functionality, is publicly available (Duffell 2016a,b).

As in Farris et al. (2014, 2015), the simulation domain in each run covers 0 < r < 100a. This is sufficiently large so that our results are not affected by the outer boundary conditions. Outside the cavity, the radial grid spacing increases approximately logarithmically, allowing us to concentrate computational resources on the flow in the inner regions of the disc. Inside the cavity, the grid spacing is roughly linear with $dr \sim 0.02a$. At all radii, we chose our azimuthal grid spacing such that the aspect ratio of each cell is kept approximately unity, unless this requires a number of azimuthal grid cells $N_{\phi} > 384$, in which case we cap the number of ϕ -zones and set $N_{\phi} = 384$.

Our initial disc configuration is similar to that in Farris et al. (2015). We modify the standard steady-state Shakura–Sunyaev disc

profile by exponentially reducing the density and pressure at small radii by a factor of $\exp[-(r/r_0)^{-10}]$ to create a hollow cavity within $r_0 \equiv 2.5a$,

$$\Sigma(r) = \Sigma_0 \exp[-(r/r_0)^{-10}]r^{-0.5}.$$
 (1)

We do not include self-gravity; this assumption is justified for compact binaries in the inner regions of the disc. As a result, the normalization of the surface density Σ_0 does not affect the simulation and is arbitrary. For convenience, we set $\Sigma_0 = 1$ in code units.

We simulate the hydrodynamical evolution of a thin circumbinary disc by solving the vertically averaged 2D Navier–Stokes equations. The pressure is set to enforce a locally isothermal equation of state of the form

$$c_{\rm s} = (h/r)\sqrt{\frac{M_1}{r_1} + \frac{M_2}{r_2}}. (2)$$

Throughout this work, we choose h/r = constant = 0.1. We employ a standard α -law viscosity (Shakura & Sunyaev 1973) of the form $v = \alpha c_s^2 \Omega_k^{-1}$, with $\alpha = constant = 0.1$ (see appendix A in D'Orazio et al. 2013; Farris et al. 2014 for detailed descriptions of the viscosity implementation in polar coördinates).

In each of our simulations, we assume that the disc mass is small compared to the binary mass, $M_{\rm disc} \ll M_{\rm bin}$ so that we may neglect the self-gravity of the gas, as well as changes in the binary's orbital elements due to torques from the gas. In this work, we further focus on the equal-mass binary case (q = 1).

In order to ensure that a quasi-steady state has been established over the spatial region of interest in our simulations, we evolve the system for 2.5 viscous time-scales at the radius of the cavity wall at $r \approx 2a$,

$$t_{\rm vis} = \frac{2}{3} \left[\alpha \left(\frac{h}{r} \right)^2 \Omega(r) \right]^{-1} \sim 300 \left(\frac{r}{2a} \right)^{3/2} t_{\rm bin}, \tag{3}$$

where $\Omega(r)$ is the Keplerian angular frequency in the disc at the radial distance r from the binary's centre of mass and $t_{\rm bin}$ is the binary's orbital period.

2.2 Accretion prescription

To mimic accretion on to the individual BHs, we follow the sink prescription used in Farris et al. (2014, 2015), but with some refinements. At each time-step, the gas surface density in cells within a distance $r_{\rm sink}$ (measured from each individual BH) is reduced uniformly by a fraction $\frac{dr}{\tau_{\rm sink}}$, where dt is the time-step, and the sink time-scale $\tau_{\rm sink}$ is a parameter to control the mass-removal rate, defined as

$$\left(\frac{\mathrm{d}\Sigma}{\mathrm{d}t}\right)_{\mathrm{sink}} \equiv -\frac{\Sigma}{\tau_{\mathrm{sink}}}.\tag{4}$$

In this work, we use $r_{\rm sink} = 0.1a$ as the fiducial value. In our previous work (Farris et al. 2014), $\tau_{\rm sink}$ was set at the local viscous time based on the α viscosity law, applied to the individual minidiscs,

$$t_{\text{vis}} = \frac{2}{3} \frac{r^2}{\nu} = \frac{1}{3\pi} \frac{1}{\alpha (h/r)^2} \left(\frac{r}{a}\right)^{3/2} u^{-1/2} t_{\text{bin}}.$$
 (5)

Here, r is the distance to each individual accreting BH (analogous to equation 3 for the circumbinary disc), u = 1/2 is the ratio of the BH mass to the total binary mass and $t_{\rm bin}$ is the binary orbital period (which is 2π in code units).

In this work, we choose τ_{sink} to be a constant inside the sink radius, and perform a suite of simulations with a range of values

of $au_{\rm sink}$. This allows us to examine the relationship between the binary–disc torques and the mass-removal rate in the sink. When we model the minidisc as a thin lpha disc, we adopt $au_{\rm sink} = t_{\rm vis}(r_{\rm sink})$ as the sink time-scale.

2.3 Measuring torques

In our simulations, the mass and velocity of the BH binary are both fixed. In other words, we calculate the torque exerted on the BHs by the circumbinary disc, but do not include the impact of these torques on the binary's orbital elements. This is justified as long as the torques are small enough so that the binary's orbit does not evolve during the simulation.

The binary's total angular momentum L changes as a result of gravitational torques and from accretion,

$$\frac{\mathrm{d}L}{\mathrm{d}t} = \frac{\mathrm{d}(M_{\mathrm{bin}}\ell)}{\mathrm{d}t} = \sum_{\mathrm{cells}} \boldsymbol{r}_{\mathrm{bh}} \times \boldsymbol{f}_{\mathrm{gr}} + \sum_{\mathrm{sink}} \boldsymbol{r}_{\mathrm{bh}} \times \dot{m}_{i} \boldsymbol{v}_{i}, \tag{6}$$

where ℓ denotes the specific angular momentum of the binary and $M_{\rm bin} = M_1 + M_2$ is the total binary mass ($M_{\rm bin} \equiv 1$ in code units, as stated above).

For convenience, we here define all torques T_i such that $T_i/M_{\rm bin}$ denotes the rate of change of the binary's specific (rather than total) angular momentum,

$$T_{\text{tot}} \equiv M_{\text{bin}} \frac{\mathrm{d}\ell}{\mathrm{d}t} = \frac{\mathrm{d}(M_{\text{bin}}\ell)}{\mathrm{d}t} - \dot{M}\ell \tag{7}$$

$$= \sum_{\text{calls}} \mathbf{r}_{\text{bh}} \times \mathbf{f}_{\text{gr}} + \sum_{\text{sink}} \mathbf{r}_{\text{bh}} \times \dot{\mathbf{m}}_{i} (\mathbf{v}_{i} - \mathbf{v}_{\text{bh}})$$
(8)

$$\equiv T_{\rm gr} + T_{\rm acc}.\tag{9}$$

The gravitational torque is given by numerically summing the gravitational force $f_{\rm gr}$ exerted by the fluid elements in each computational cell on the individual BHs,

$$T_{\rm gr} = \sum_{\rm calls} \mathbf{r}_{\rm bh} \times \mathbf{f}_{\rm gr}. \tag{10}$$

For the accretion torque, we measure the linear momentum of the gas removed in each simulation cell inside the sink, relative to the accreting BHs,

$$T_{\rm acc} = \sum_{\rm sink} \mathbf{r}_{\rm bh} \times \dot{m}_i(\mathbf{v}_i - \mathbf{v}_{\rm bh}), \tag{11}$$

where v_i and v_{bh} are the velocities of the gas and of an individual BH (as measured in the inertial frame). Note that this definition differs by the term $-\dot{M}\ell$ from the accretion torques in Roedig et al. (2012) and Dürmann & Kley (2017).

Throughout this work, the binary BHs have equal mass and are fixed on a circular orbit, so that its specific angular momentum is

$$\ell = \sqrt{GM_{\rm bin}a}/4. \tag{12}$$

Differentiating equation (12), we obtain the binary residence time

$$t_{\rm res}^{-1} \equiv -\frac{\dot{a}}{a} = -\left(\frac{2\dot{\ell}}{\ell} - \frac{\dot{M}}{M_{\rm bin}}\right). \tag{13}$$

3 RESULTS

Snapshots of the surface density from simulations with fast $(\tau_{\text{sink}} = 0.0125 \text{ or } 0.002t_{\text{bin}})$ and slow $(\tau_{\text{sink}} = 5.0 \text{ or } 0.64t_{\text{bin}})$ mass-removal rate are shown in Fig. 1. As discussed below, the former sink is unphysically fast and represents a numerical experiment;

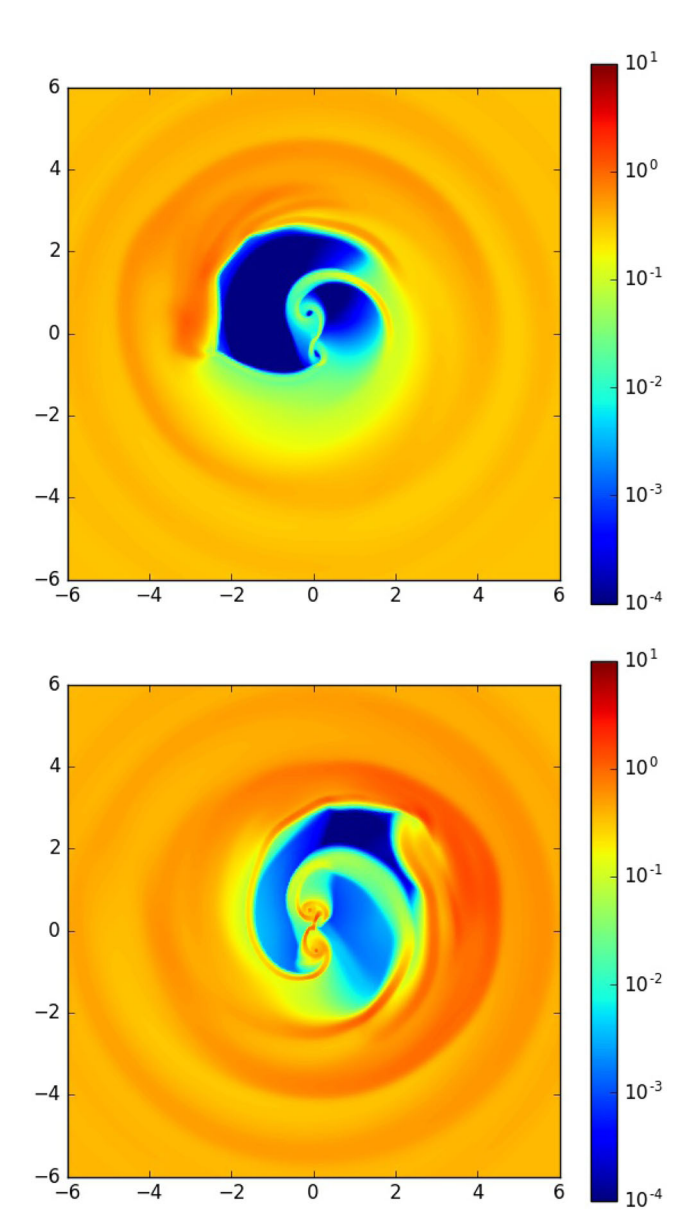


Figure 1. Snapshots of the surface density Σ at $t \approx 800 t_{\rm bin}$. The contours show Σ in units of the initial Σ_0 , on a logarithmic scale indicated by the side-bars. The x/y axes are in units of binary separation. The orbital motion of both the binary and the disc are in the counterclockwise direction. The upper panel is for a rapid sink (with mass-removal time-scale $\tau_{\rm sink} = 0.0125$ or $0.002 t_{\rm bin}$), whereas the lower panel is for a slower sink ($\tau_{\rm sink} = 5.0$ or $0.64 t_{\rm bin}$). $t_{\rm bin} = 2\pi$ in code units.

the latter value is chosen to correspond to $\alpha=0.59$. In both cases, we confirm the findings in many previous studies (beginning with Artymowicz & Lubow 1994, 1996 and with recent works including, e.g. MacFadyen & Milosavljević 2008; Cuadra et al. 2009; Shi et al. 2012; Noble et al. 2012; Roedig et al. 2012; D'Orazio et al. 2013; Farris et al. 2014), namely that a low-density, lopsided cavity forms around the binary, while narrow accretion streams connect the cavity wall to the minidiscs around the individual BHs. Most of the material in the narrow streams does not accrete on to a BH, but rather is flung outwards. The outward-going streams create an overdense lump at the cavity wall. As the figure shows, the more rapid sink (top panel) depletes the gas near the BHs, as well as in the entire inner region of the circumbinary disc, compared to the slower sink (bottom panel).

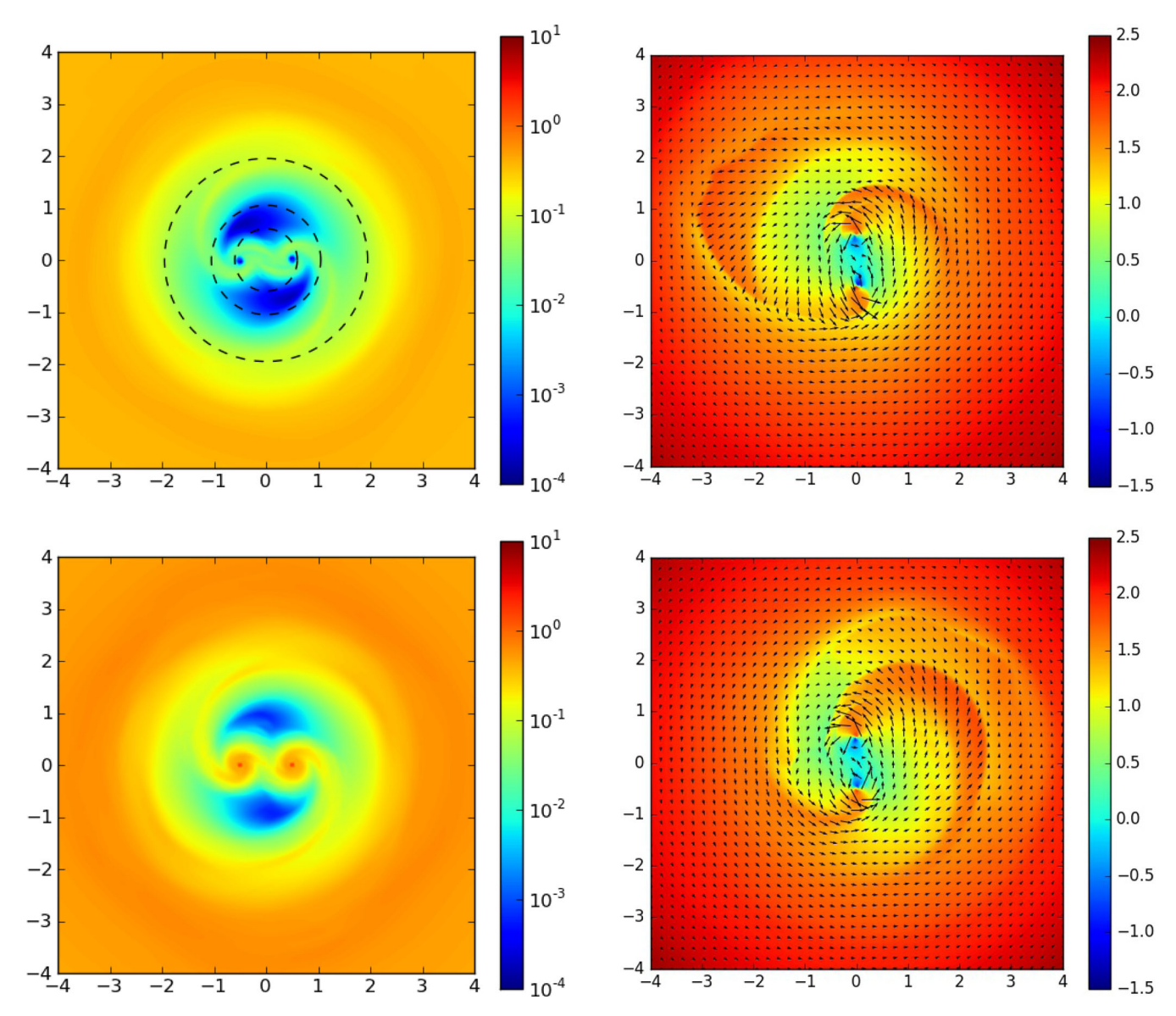


Figure 2. Time-averaged surface density profiles. Time-averaging is taken over \sim 100 orbits, and in a corotating frame where the BHs are at the fixed coordinates (-0.5,0) and (+0.5,0). As in Fig. 1, the upper (lower) panel is for a rapid (slower) sink, with a mass-removal time-scale of $\tau_{\rm sink} = 0.0125$ [5.0]. The three dashed circles have radii of 0.6, 1.05 and 1.95a, and demarcate annular regions in which the net gravitational torques switch sign from positive (0.6 < r < 1.05) to negative (1.05 < r < 1.95).

In Fig. 2, we show the time-averaged surface density profiles in a frame corotating with the binary. We find again that with a faster sink, the surface density of the minidiscs, of the accretion streams, and of the circumbinary discs near the cavity wall, are all visibly reduced. The three dashed circles in the top panel have radii of 0.6, 1.05 and 1.95a. In the annulus between the latter two circles, the azimuthal phase of the accretion stream trails behind the binary. As a result, the gravitational force between the binary and these portions of the accretion streams exert a negative torque on the binary (as further illustrated in Fig. 4 below). By comparison, in the annulus between the first two circles, the tails of the narrow streams are ahead of the individual BHs, and therefore exert a positive gravitational torque on the binary. Comparing the shape of the minidiscs in the top and bottom panels, we find that the minidiscs in the fast-sink case are

Figure 3. Snapshots of the distribution of specific angular momentum $|r \times v|$. The snapshots are taken from the same runs and at the same time as in Fig. 1, and as in the previous figures, the top (bottom) panel is for a fast (slow) sink. Black arrows denote the local velocity field for the disc gas. The prominent streams travel outwards, and carry angular momentum from the binary to the circumbinary disc.

less dense overall; they are furthermore less round and symmetric than in the slow-sink case. Finally, an important conclusion from this figure is that the fast sink preferentially depletes the gas density behind (versus ahead of) the individual BHs (i.e. in the annulus 0.6 < r < 1.05).

As discussed in several previous works (MacFadyen & Milosavljević 2008; Roedig et al. 2012; Shi et al. 2012; D'Orazio et al. 2013; Farris et al. 2014), most of the material in the narrow streams gains angular momentum from the faster moving BHs and is flung back towards the cavity wall. In Fig. 3, we plot contours of specific angular momentum in runs with both fast and slow sinks (top and bottom panel, respectively). These confirm that the specific angular momentum of the material forming the narrow streams is larger than that of the cavity wall, and also that overall, the streams have a net outward-going velocity. This suggests that the narrow

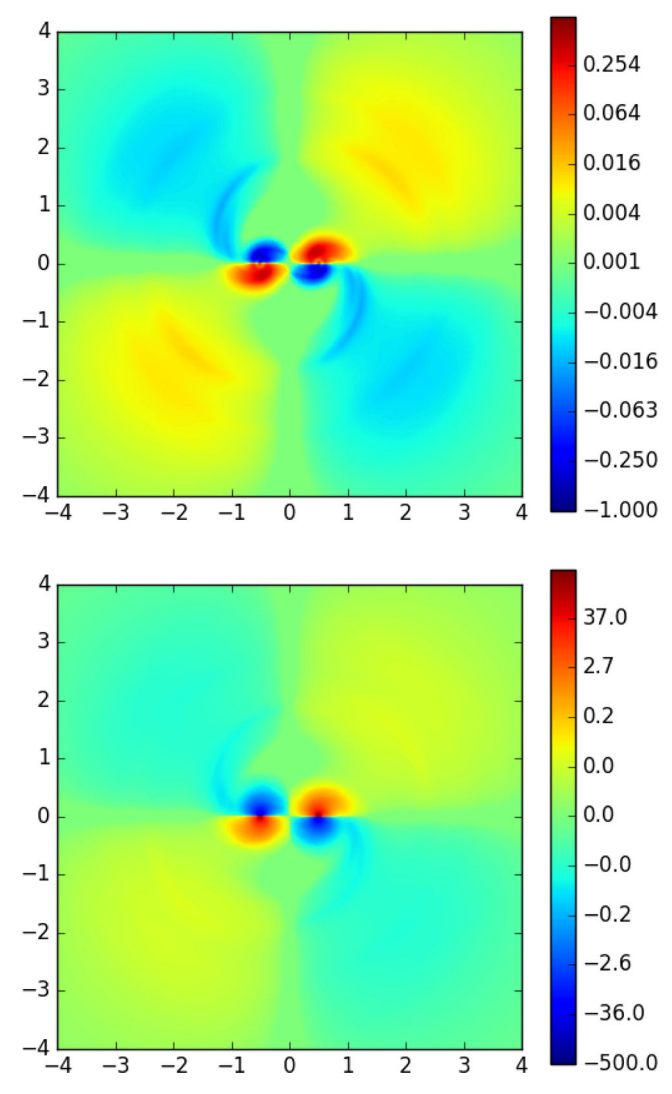


Figure 4. Time-averaged distributions of the gravitational torque surface density exerted by the gas disc on the binary. The sink time-scales in the top and bottom panels are $\tau_{\rm sink} = 0.0125$ and 5.0, as in previous figures. The net torque is positive in the top panel and negative in the bottom panel. Note the different scales in the two panels.

streams could extract angular momentum from the binary and deposit it into the circumbinary disc, effectively acting as media to carry angular momentum from the binary to the gas disc.

In Fig. 4, we plot the 2D distribution of the gravitational torque surface density, and in Fig. 5, we plot the radial distribution of the azimuthally averaged gravitational torque density. The previous works by MacFadyen & Milosavljević (2008) and Farris et al. (2014) calculated the torques only in the region r > 1.0a. Our results are qualitatively similar to these studies in this region. In particular, we find significant negative torques from the disc material in the annulus between a < r < 2a, corresponding to the extended faint blue streams in Fig. 4. The total torque from the outer regions r > a is also negative, with r > 3a contributing negligibly to this total. However, we find a significant positive torque in the annulus 0.6a < r < a. Fig. 4 further quantifies the point mentioned above, namely that this positive torque can be attributed to the compact tails of the narrow streams. These can be seen as the prominent red clumps in the figure, located near and ahead of the individual BHs. In the fast-sink case, the contribution from this region dominates,

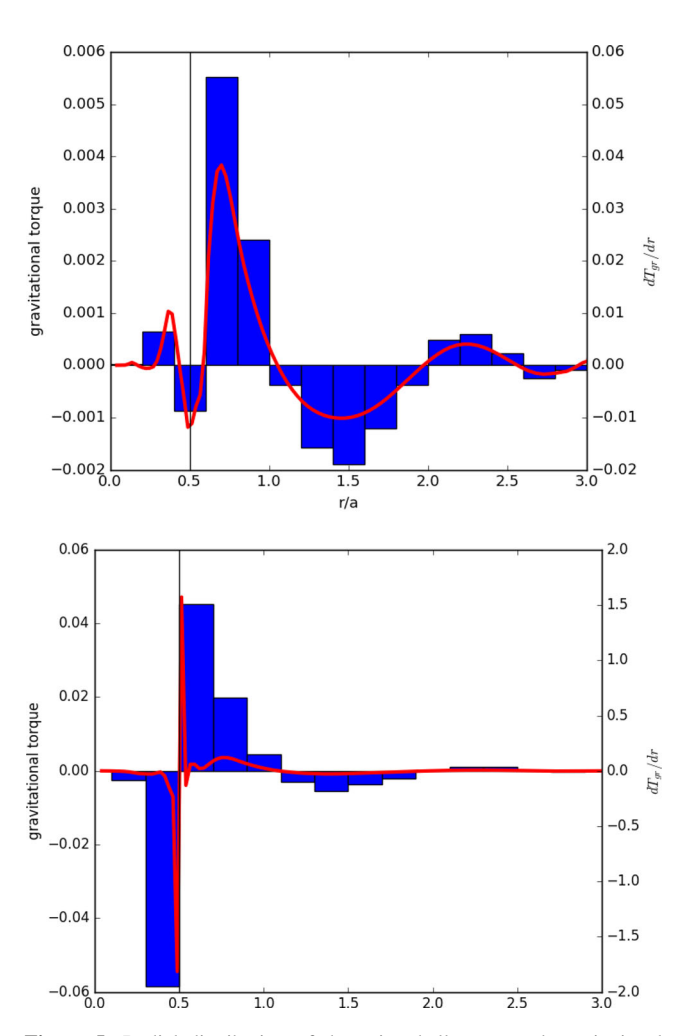


Figure 5. Radial distribution of the azimuthally averaged gravitational torque density $dT_{\rm gr}/dr$, corresponding to the runs in Fig. 4. The red curve shows the torque density with corresponding *y*-axis labels on the right. The blue histogram shows the contributions to the torque in wider finite radial bins, with the corresponding *y*-axis labels on the left. The vertical line shows the location of the BH. The contribution from the region r > 3a is negligible in all of the runs. The net gravitational torques are 0.3 and $-0.68 \ \dot{M}$ in the top and bottom panels, respectively.

making the total torque positive. In the slow-sink case, the negative torques from the more massive minidiscs roughly cancel the positive torques from the tails of the narrow streams, and the result is a net negative torque.

In Fig. 6, we plot the radial angular momentum flux profiles for both fast and slow sinks. We show separately the fluxes corresponding to advection $(\int_0^{2\pi} r^2 \rho v_r v_\phi d\phi)$; blue curve), viscosity $(\int_0^{2\pi} T_{\phi r}^{\rm vis} d\phi)$ with $T_{\phi r}^{\rm vis} = -\rho v r^2 \nabla_r \Omega$; green) as well as the gravitational torques $(-\int_0^r dT_{\rm gr})$; cyan). The details of the numerical implementation of these fluxes in DISCO can be found in Duffell & MacFadyen (2013). The accretion torques are not shown explicitly, but correspond to a source term near the BHs (they are negligible in the lower panel, but account for the visible constant offset between the red and cyan curves at $r \approx 0.6$ in the upper panel). With the fast sink, the net torque exerted on the binary is positive, implying that angular momentum is transported from the disc to the binary. With the slow sink, the situation is the reverse, and angular momentum is transported outwards from the binary to the disc.

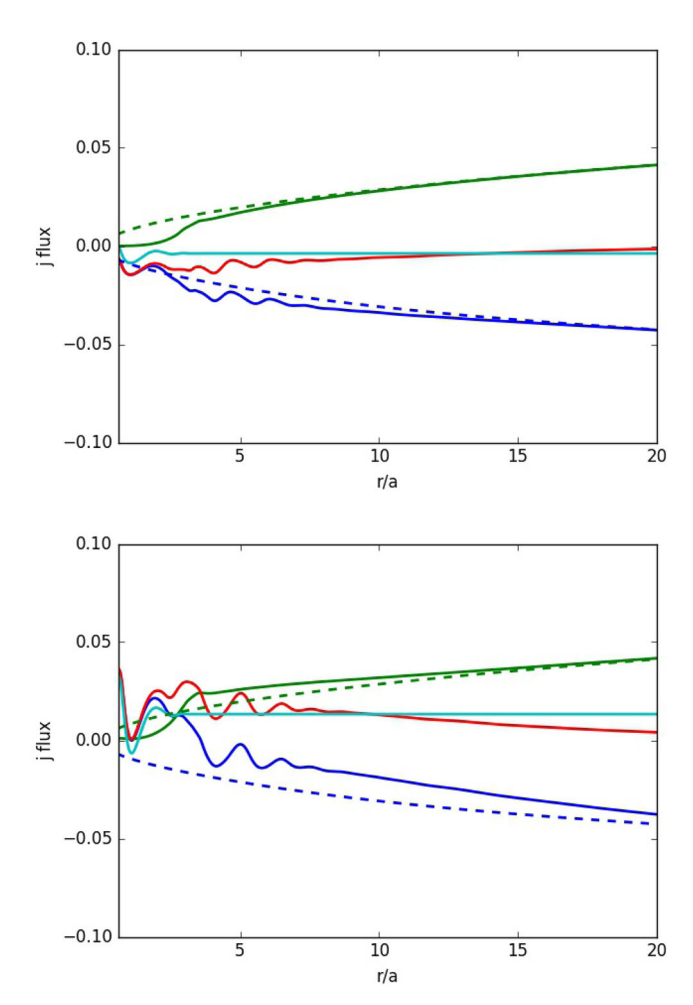


Figure 6. Radial profiles of angular momentum flux for a fast (top; $\tau_{\rm sink}=0.0125$) and slow sink (bottom panel; corresponding to $\alpha=0.1$). The fluxes corresponding to viscosity, gravitational torques and advection are shown by the green, cyan and blue curves, respectively. The red curve is the sum of the green and blue curves. The dashed curves show the viscous and advected fluxes in a reference single-BH simulation with the same BH mass and disc parameters. In the bottom panel, the binary is loosing angular momentum to the disc, with this excess angular momentum transported outwards by enhanced viscosity (at $r\gtrsim 3a$). In the top panel, the binary is gaining angular momentum from the disc, with reduced viscosity allowing net inward angular momentum transfer.

We find that inside the cavity, the viscous angular momentum flux is close to zero, and advection is the only effective way to transfer angular momentum. With a slow sink, the advected angular momentum flux turns positive in the cavity. This implies that the narrow streams in the cavity are able to carry angular momentum outwards to the cavity wall. When compared to the analogous results from a single-BH reference disc (shown by the dashed curves), we find that both the viscous and advected fluxes shift up or down based on the direction of the net angular momentum flux. However, at large radii, the viscous flux converges to the single-BH solution faster than the advected flux.

Overall, we conclude that when the net torque on the binary is negative (bottom panel), the angular momentum of the binary ends up being deposited into the circumbinary disc, and transported outwards first by gravitational torques and advection (in the inner regions; $r \lesssim 3a$) and then by the elevated viscosity (farther out; $r \gtrsim 3a$). For the fast sink (top panel), the behaviour is the opposite,

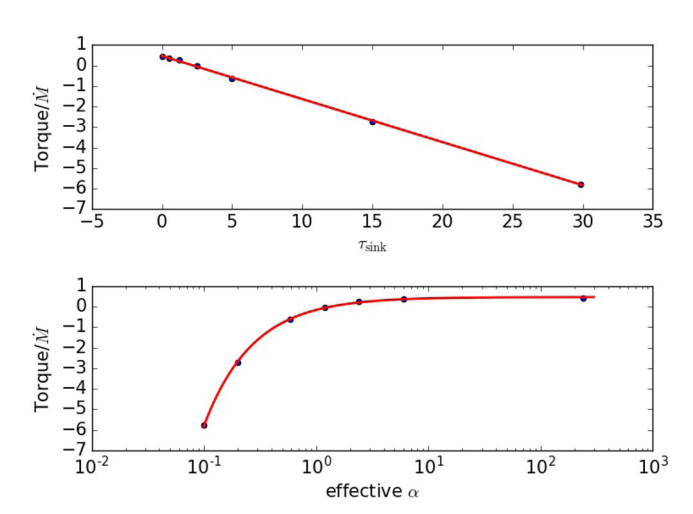


Figure 7. Top panel: total specific torque on the binary, in units of \dot{M} , as a function of the sink time-scale $\tau_{\rm sink}$. The red line is a best fit to the simulation results (black points), and has a slope and intercept of -0.21 and 0.47, respectively. Bottom panel: total torque as a function of the effective viscosity parameter α (calculated from equation 5).

with reduced viscosity enhancing the inward advection of angular momentum, which ultimately results in a net transfer of angular momentum from the disc on to the binary.

In Fig. 7, we show the net specific torque on the binary, in units of \dot{M} , as a function of the sink time-scale $\tau_{\rm sink}$. We find a clear linear relationship with longer sink time-scales yielding more negative specific torque. The total torque exerted on the binary is well approximated by the equation:

$$T_{\text{tot}} = (-0.21\tau_{\text{sink}} + 0.47)\dot{M}.\tag{14}$$

When $\tau_{\rm sink}$ is below a critical value of $\tau_{\rm sink,\,crit}=2.1$, the binary feels a net positive torque from the gas disc. In the bottom panel of Fig. 7, we show the total torque as a function of the corresponding effective α (using equation 5 to convert $\tau_{\rm sink}=t_{\rm visc}$ to α). The effective viscosity parameter corresponding to $\tau_{\rm sink,\,crit}=2.2$ is $\alpha_{\rm crit}=1.36$. We conclude that for sink time-scales corresponding to physically realistic choices of viscosity, binaries are always driven towards merger, rather than pushed apart, by the presence of the circumbinary gas disc.

Kocsis, Haiman & Loeb (2012a,b), Rafikov (2013) and recently Rafikov (2016) have used simplified 1D models to study how the surface density profile of a steady accretion disc responds when angular momentum is injected to (or extracted from) an α disc at some small radius by a binary companion (see also Syer & Clarke 1995 for related earlier work). These analytic 1D steady-state solutions resemble standard Shakura–Sunyaev discs, but the disc adjusts itself to transfer angular momentum outwards (or inwards) at the same rate as the injection (or extraction) rate imposed at the bottom (i.e. at a small radius, comparable to the binary separation). These modified angular momentum transfer rates require a surface density 'pile-up' (or depletion) in the inner disc regions.

The form of this modified disc profile can be approximated by combining equations 3 and 11 of (Rafikov 2016, see also his fig. 2). The modified surface density follows the form

$$\Sigma(r) = A/\sqrt{r} - B/r,\tag{15}$$

where A and B are constants, related to one another as

$$B/A = \dot{J}/\dot{M}. \tag{16}$$

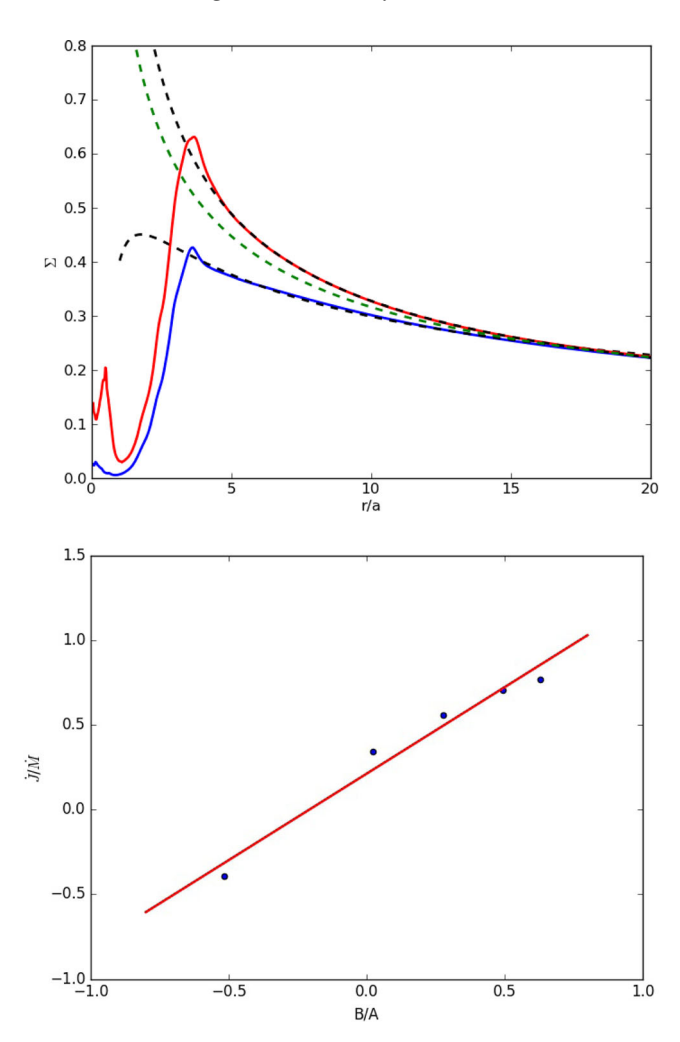


Figure 8. Time-averaged surface density profiles and best-fitting analytic curves. The red and blue curves in the top panel correspond to the fast and slow sinks, respectively. The black dashed curves follow $\frac{A}{\sqrt{r}} - \frac{B}{r}$, where A and B are free parameters fit to the simulated profiles. The green dashed line denotes the unmodified profile \sqrt{r} . The bottom panel shows the relationship between $\langle \dot{J}/\dot{M} \rangle$ and the ratio B/A of the best-fitting values. The straight red line is a least-squares fit to the simulation results (shown by black points), and has a slope of \sim 1.02 and intercept \sim 0.21. These are in good agreement with the predictions of 1D steady-state models for how the disc responds to binary torques (see the text for discussion).

Here, \dot{J} is the angular momentum flux absorbed by the binary (which can be either negative or positive) and \dot{M} is the mass accretion rate that is always positive.

In Fig. 8, we show the time-averaged and azimuthally averaged surface density profiles from our simulations, for both a fast (top panel) and a slow sink (bottom panel). We find that outside the cavity wall, in the region 5a < r < 15a, $\Sigma(r)$ differs from the initial condition $1/\sqrt{r}$ (green dashed line) and accurately follows the form given in equation (15). In Fig. 8, we further test the 1D predictions, and plot the empirical relationship between $\langle \dot{J} \rangle / \langle \dot{M} \rangle$ and the B/A value obtained from fitting the profiles found in the simulations. We find

$$\frac{\langle \dot{J} \rangle}{\langle \dot{M} \rangle} = 1.02 \left(\frac{B}{A} \right) + 0.21,\tag{17}$$

which matches the prediction (equation 16) quite well. Nevertheless, we caution that in order to reach a steady state throughout the

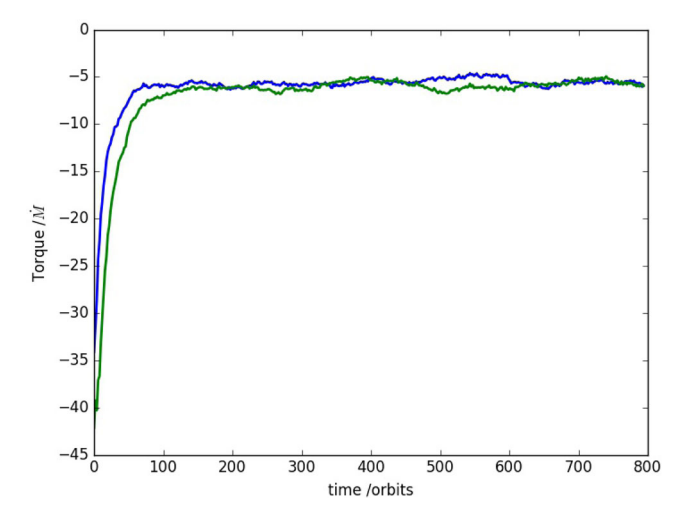


Figure 9. Moving time-averaged total torque versus time with two different choices of sink radius. The blue curve is for $r_{\rm sink} = 0.05a$ and the green curve is for $r_{\rm sink} = 0.1a$. The time-averaging window is 60 orbits. The torques converge rapidly to a value that is insensitive to the choice of $r_{\rm sink}$.

disc, we would need to run the simulations for several viscous times measured at the outermost disc radius. Thus, Fig. 8 should be interpreted only as evidence for a 'temporary' steady state in the inner regions, and for the sink time-scale affecting the global surface density structure as expected, rather than a prediction for the long-term steady-state surface density profile, which would be established on a much longer time-scale.

Ryan & MacFadyen (2017) have performed a general relativistic local simulation of an isolated minidisc, subject to the tidal field of a companion. Their simulation does not include gas viscosity, but shows gravitational torques arising from non-axisymmetric structures (spiral waves) inside the minidisc, induced by the tidal torques of the companion BH. They find that the minidisc has an effective 'gravitational Shakura–Sunyaev α ' on the order of a few \times 10^{-2} . Since this effect does not significantly enhance the effective α parameter of the minidisc, we proceed to assume the physical sink time-scale $\tau_{\rm sink}$ equals the viscous time at $r_{\rm sink}$.

To investigate whether the sink radius $r_{\rm sink}$ affects our results, we have performed simulations with $r_{\rm sink}=0.1a$ and 0.05a. In each case, we have set the sink time-scale to $\tau_{\rm sink}=t_{\rm vis}(r_{\rm sink})$. Fig. 9 shows the specific torque, in units of \dot{M} , as a function of time in these two simulations. The figure shows that the torques converge rapidly to a value that is insensitive to the choice of $r_{\rm sink}$. In both runs, we find that the gravitational torque dominates over the accretion torque, with $|T_{\rm acc}|/|T_{\rm tot}|\approx 0.01$.

In summary, in Table 1 we list the simulation parameters and the gas disc torques exerted on the binary in each of our simulations.

4 DISCUSSION

4.1 Implications for the SMBH binary population

In our simulations, the binary orbital period is 2π , and the accretion rate \dot{M} is arbitrary, depending linearly on the surface density normalization Σ_0 . By scaling the simulation to $t_{\rm bin}=1$ yr, and $\dot{M}=0.3\,\dot{M}_{\rm Edd}$ (with $\dot{M}_{\rm Edd}\equiv L_{\rm Edd}/\epsilon c^2,\,\epsilon=0.1$ i.e. the accretion rate corresponding to the Eddington luminosity), we obtain the binary's residence time $t_{\rm res}\equiv a/[{\rm d}a/{\rm d}t]$ in physical units (equation 13). We find that this time-scale due to the gas torque is $t_{\rm res}=3.26\times10^6$ yr. We note that $t_{\rm res}\approx\ell/[{\rm d}\ell/{\rm d}t]$; the contribution

Table 1. Summary of our simulation runs. The columns, from left to right, show the (i) sink time-scale, (ii) the corresponding effective viscosity parameter, (iii) sink radius and (iv) total dimensionless specific torque.

τ_{sink}	Effective α	$r_{\rm sink}$	$T_{ m tot}/\dot{M}$
0.0125	238.51	0.1	0.433
0.5	5.96	0.1	0.373
1.25	2.38	0.1	0.269
2.5	1.19	0.1	-0.0271
5.0	0.59	0.1	-0.625
15.0	0.2	0.1	-2.724
29.84	0.1	0.1	-5.77
9.621	0.1	0.05	-5.52

from mass accretion (the second term in equation 13) is an \approx 2 per cent correction. In our code units ($M_{\rm bin}=a=1$, $t_{\rm bin}=2\pi$), the conversion constant for the accretion rate is $t_{\rm bin}/(2\pi M_{\rm bin})$. Therefore if $\dot{M}/\dot{M}_{\rm Edd}$ is fixed, in our code units \dot{M} is proportional to $t_{\rm bin}$ and independent of $M_{\rm bin}$. In code units, the residence time $\tilde{t}_{\rm res} \propto T_{\rm tot}^{-1} \propto \Sigma_0^{-1} \propto \dot{M}^{-1} \propto t_{\rm bin}^{-1}$ and the physical residence time $t_{\rm res} = \tilde{t}_{\rm res} \times t_{\rm bin}/2\pi$. Thus, the inferred residence time in physical units does not depend on $M_{\rm bin}$ or $t_{\rm bin}$. The same conclusion would follow by noting that the residence time in physical units would scale as $t_{\rm res} \propto$ (angular momentum/torque) $\propto a/(\Sigma_0 t_{\rm bin})$, with a, Σ_0 and $t_{\rm bin}$ in physical units. However, the condition $\dot{M}={\rm const}\times\dot{M}_{\rm Edd}$ implies $\Sigma_0 \propto a/t_{\rm bin}$, making $t_{\rm res}$ a constant. This counter-intuitive conclusion is a result of our scale-free simulation set-up, and would no longer hold in the presence of realistic cooling/heating or other physics introducing a physical scale.

Further choosing a total binary mass $M_{\rm bin} = 10^{6-9} \, \rm M_{\odot}$, the inspiral time-scale due to gravitational wave (GW) emission is $t_{\rm GW} = 5.2 \times 10^{8-3}$ yr (Peters 1964). We conclude that the scaled gas-driven inspiral time, implied by our simulations, is comparable to (or shorter than) the GW-driven inspiral time for binaries with total mass $M_{\rm bin} \lesssim 10^7 \, \rm M_{\odot}$.

Pulsar timing arrays (PTAs) are sensitive to \sim nHz-frequency GW generated by SMBHBs with orbital periods between \sim 0.1 and 10 yr. Because gas torques can promote orbital decay of the binary much more efficiently than pure GW emission, the expected number of binaries, and the GW background (GWB) at these separations should be reduced accordingly (Kocsis & Sesana 2011; Kelley et al. 2017). Although we find that for the 10^{8-9} M $_{\odot}$ binaries that dominate the GWB, the gas torques are subdominant, we expect the impact of the gas torques to increase for smaller mass ratios (because gas torques increase, whereas GW torques decrease, for smaller q; e.g. Haiman, Kocsis & Menou 2009). Syer & Clarke (1995, see also Kocsis et al. 2012a,b) have proposed analytical models analogous to Type-II migration, in which migration rates are tied to the disc viscous time, but are slowed down by a factor related to the ratio $M_2/M_{\rm disc}$, when this ratio is above unity.

For a steady-state α disc with $M_{\rm bin}=2\times10^{6-9}\,{\rm M}_{\odot}$, and accretion rate $\dot{M}=0.3\,\dot{M}_{\rm Edd}$, the viscous time $t_{\rm vis}$ at r=0.5a is approximately $(8\times10^4-10^6)$ yr, and the predicted residence time $t_{\rm res}$ is approximately $(50-3)t_{\rm vis}\approx(4-3)\times10^6$ yr (see Haiman et al. 2009 for a detailed calculation). This turns out to be very close to the result $t_{\rm res}\sim3\times10^6$ yr we infer here by scaling the torques measured in our simulations. We emphasize that this good agreement appears to be a coincidence, because in the 1D models, the torques are assumed to arise from the overdense cavity wall of the circumbinary disc, whereas in our simulations, the torques are dominated by the gas near the individual BHs.

We note further that a steady-state α disc with an accretion rate of $0.3\,\dot{M}_{\rm Eedd}$ has a scaleheight of $H/r\sim 10^{-3}$, and is much thinner than the disc in our simulations (H/r=0.1). While simulating discs numerically with $H/r\sim 10^{-3}$ is currently prohibitively challenging, our choice of H/r=0.1 is typical for the values employed in previous works (Artymowicz & Lubow 1994; MacFadyen & Milosavljević 2008; D'Orazio et al. 2013; Farris et al. 2014) and allows for a direct comparison with those works. We expect that the dimensionless torques measured in the simulations will depend on H/r, and we intend to investigate this dependence in future work.

We have found that the sink prescription and time-scale affect the magnitude (and even the sign) of the torques on the binary. Slower sinks result in more negative torques on the binary, while faster sinks result in diminished negative (or even positive) torques. During the late stages of the merger, the Schwarzschild radius $r_{\rm S}$ is not much smaller than the binary separation. A more physically realistic sink prescription during this stage would be to adopt the dynamical time as the sink time-scale $\tau_{\rm sink}$, and the innermost stable circular orbit ($r_{\rm ISCO}$) as the sink radius $r_{\rm sink}$. However, a more careful treatment of relativistic effects, e.g. through the use of the Paczynski–Wiita potential (Paczyńsky & Wiita 1980) is required in this case.

4.2 Comparison with previous works

The nature of the torques and the corresponding binary evolution, arising from the disc-binary interaction, has been previously investigated by Cuadra et al. (2009), Roedig et al. (2012) and Miranda et al. (2017) as mentioned in the Introduction. Cuadra et al. (2009) and Roedig et al. (2012) have both simulated self-gravitating gaseous discs of mass $M_{\rm disc}=0.2\,M_{\rm bin}$ and BH mass ratio q=1/3. The disc is Toomre unstable, and self-gravity acts as a source of viscosity that can transport angular momentum outwards. In their SPH simulations, gas particles in the sink are absorbed by the BH immediately, which corresponds to a sink time-scale $\tau_{\rm sink}=0$. Similar to our results, Roedig et al. (2012) find that the gravitational torque changes sign at r=a (positive at r < a and negative at r > a).

They also find that accretion (of mass and angular momentum) alone would shrink the binary separation significantly. In our work, the accretion torque is positive, but is generally very weak. We find that the contribution from accretion (of mass and angular momentum) reduces the binary orbit (once both terms in equation 13 are included), in agreement with the sign in Roedig et al. (2012), but we find accretion to be unimportant compared to gravitational torque (an order of 10^{-2} correction). In comparison, in Roedig et al. (2012), the binary is driven together by the disc with a residence time of approximately 8000 binary orbits (taking their run closest to ours, i.e. 'iso10' in their fig. 3).

In Roedig et al. (2012), the typical accretion rate is much higher than the Eddington rate (20–40 $\dot{M}_{\rm Edd}$ for the secondary and 4–7 for the primary when $M_{\rm primary}=2\times 10^6\,{\rm M}_{\odot}$ and $a=0.039\,{\rm pc}$). We have found that the total torque exerted on the binary sensitively depends on the sink time-scale, and with a fast sink the binary is driven apart by the gas. If we re-scale our simulations to the same \dot{M} , $M_{\rm bin}$ and separation a, and we adopt $\tau_{\rm sink}=t_{\rm visc}$, the residence time we obtain is approximately 250 binary orbits, which is around 30 times smaller. This difference may come from the different binary mass ratio, equation of state, disc thickness, as well as from the effect of self-gravity as well as from the different duration of the runs (Roedig+2012 run their simulations for 90 orbits, whereas we run them for approximately 1000 orbits). Moreover, we suspect that for a more physical (i.e. less rapid) sink prescription was employed,

the migration rate $-\frac{da}{dt}$ in Cuadra et al. (2009) and Roedig et al. (2012) would be faster, and closer to our value.

Finally, we note that Miranda et al. (2017) perform a series of 2D viscous hydrodynamics simulations of circumbinary discs, but with the inner regions (r < a) excised from the simulation domain. They conclude that the binary feels a net positive torque. This positive torque arises from accretion, and is a direct result of the assumption that the specific angular momentum of the disc gas near $r \approx a$ ends up being accreted by the binary. As we have seen in our simulations that resolve the inner regions, this is not the case. Rather than being deposited into the binary, the large angular momentum of this gas is returned to the disc, via narrow streams, in a 'gravitational slingshot' mechanism.

4.3 Caveats and future work

In future work, we intend to relax several assumptions, while expanding the parameter space of our simulations. In this paper, we have focused on a mass ratio q = 1, viscosity $\alpha = 0.1$, and disc aspect ratio H/r = 0.1. In the future, we intend to study how these parameters affect the torques and the evolution of the binary's orbital parameters. In this paper, we have further assumed a locally isothermal equation of state, with the temperature set to the same value for the circumbinary disc and for both minidiscs. This assumption should be relaxed by incorporating a more sophisticated treatment of the thermodynamics, so that the minidiscs are allowed to heat or cool independently (e.g. Farris et al. 2015). Realistic circumbinary discs will also have a range of thicknesses, and we intend to investigate the dependence of gas torque on H/r (e.g. Ragusa, Lodato & Price 2016). In this paper, the binary moves on a fixed, prescribed circular orbit. In future work, this assumption should also be relaxed, in order to measure the growth of eccentricity due to the binary-torque interaction (e.g. Cuadra et al. 2009) and selfconsistently couple the evolution of the binary and the disc (e.g. Dürmann & Kley 2017). If significant eccentricity is imparted to the binary, it may have observational consequences for GW observations, especially for the GWB measured by PTAs. Finally, our simulations are in 2D. We expect that the 3D vertical structure will modify the structure of the minidisc and the accretion streams, and inevitably have a strong affect on the gas torques.

5 CONCLUSIONS

We have performed hydrodynamic simulations of thin, circumbinary accretion discs using a moving-mesh, finite-volume code with the BHs present on the simulated grid. Our discs are locally isothermal, corotating in the plane of the binary, and we employ an α viscosity prescription. The binaries follow a fixed, prescribed circular orbit. We carried out a detailed study of the gas torques exerted on the BHB. We performed a numerical experiment, to study the effect of the mass-removal rate in the sink prescription used to model accretion on to the individual BHs, on both the gas torques and on the global circumbinary disc structure. The most important conclusions of this work can be summarized as follows.

(1) We find a strong reciprocal relationship between the mass-removal time-scale and the torques on the binary. The total torque is positive when the mass-removal time-scale $\tau_{\rm sink}$ is $\lesssim 2.5$. For slower sinks, gas accumulates near the BHs and generates large negatives torques, making the net total torque exerted on the binary negative. The relationship between $\tau_{\rm sink}$ and total gas torque $T_{\rm tot}$ can be well approximated by a linear regression. When we model the minidiscs

as thin α discs, and adopt a viscous time as the sink time-scale, the gas torque exerted on the binary is always negative for $\alpha \leq 1$, and insensitive to $r_{\rm sink}$.

- (2) The gas torques are predominantly gravitational, and determined by gas dynamics near individual BHs. The gas torques come from three regions: the narrow streams, tails of the narrow streams near the minidiscs and the minidiscs themselves. The tail of the narrow stream contributes positive torque, while the other regions contribute negative torque. Rapid sinks make the tail of the narrow streams dominate, and result in a net positive total torque. For slower sinks, the negative torque from the material in the minidiscs behind the BHs cancel the positive torques from the gas ahead of the BHs, and result in a net negative torque. When we adopt the viscous time as the sink time-scale, the accretion torque is slightly positive and is at most a few per cent of the total torque.
- (3) When simulations are scaled to physical units, we find that binaries are driven together on a time-scale of $t_{\rm res} = a/|{\rm d}a/{\rm d}t| \sim 3 \times 10^6$ yr. This time-scale would be independent of $M_{\rm bin}$ or $t_{\rm bin}$, if the dimensionless torques were independent of the disc aspect ratio H/R. However, this is unlikely, and the migration rates will in general depend on H/R (and then also on $M_{\rm bin}$ or $t_{\rm bin}$). Our current results suggest that the scaled gas-driven inspiral time is comparable to (or shorter than) the GW-driven inspiral time for binaries with total mass $M_{\rm bin} \lesssim 10^7\,{\rm M}_{\odot}$. However, the above dependences, as well as the caveats listed in the previous section, will have to be explored in future work, in order to accurately assess the impact of gas torques on the binary population.

ACKNOWLEDGEMENTS

We thank Daniel D'Orazio, Paul Duffell and Geoff Ryan for useful discussions. Financial support was provided from NASA through the ATP grant NNX15AB19G (ZH). ZH also gratefully acknowledges support from a Simons Fellowship for Theoretical Physics.

REFERENCES

Artymowicz P., Lubow S. H., 1994, ApJ, 421, 651

Artymowicz P., Lubow S. H., 1996, ApJ, 467, L77

Begelman M. C., Blandford R. D., Rees M. J., 1980, Nature, 287, 307

Cuadra J., Armitage P. J., Alexander R. D., Begelman M. C., 2009, MNRAS, 393, 1423

D'Orazio D. J., Haiman Z., MacFadyen A., 2013, MNRAS, 436, 2997

Dotti M., Sesana A., Decarli R., 2012, Adv. Astron., 2012

Duffell P. C., 2016a, Astrophysics Source Code Library, record ascl:1605.011

Duffell P. C., 2016b, ApJS, 226, 2

Duffell P. C., MacFadyen A. I., 2011, ApJS, 197, 15

Duffell P. C., MacFadyen A. I., 2012, ApJ, 755, 7

Duffell P. C., MacFadyen A. I., 2013, ApJ, 769, 41

Duffell P. C., Haiman Z., MacFadyen A. I., D'Orazio D. J., Farris B. D., 2014, ApJ, 792, L10

Dürmann C., Kley W., 2017, A&A, 598, A80

Escala A., Larson R. B., Coppi P. S., Mardones D., 2005, ApJ, 630, 152

Farris B. D., Duffell P., MacFadyen A. I., Haiman Z., 2014, ApJ, 783, 134
Farris B. D., Duffell P., MacFadyen A. I., Haiman Z., 2015, MNRAS, 446, L36

Goldreich P., Tremaine S., 1980, ApJ, 241, 425

Haiman Z., Kocsis B., Menou K., 2009, ApJ, 700, 1952

Ivanov P. B., Papaloizou J. C. B., Polnarev A. G., 1999, MNRAS, 307, 79

Kelley L. Z., Blecha L., Hernquist L., Sesana A., 2017, MNRAS, preprint (arXiv:1702.02180)

Kocsis B., Sesana A., 2011, MNRAS, 411, 1467

Kocsis B., Haiman Z., Loeb A., 2012a, MNRAS, 427, 2660

Kocsis B., Haiman Z., Loeb A., 2012b, MNRAS, 427, 2680

Lin D. N. C., Papaloizou J., 1986, ApJ, 309, 846

Lippai Z., Frei Z., Haiman Z., 2009, ApJ, 701, 360

MacFadyen A. I., Milosavljević M., 2008, ApJ, 672, 83

Mayer L., 2013, Class. Quantum Grav., 30, 244008

Miranda R., Muñoz D. J., Lai D., 2017, MNRAS, 466, 1170

Noble S. C., Mundim B. C., Nakano H., Krolik J. H., Campanelli M., Zlochower Y., Yunes N., 2012, ApJ, 755, 51

Orosz J. A. et al., 2012, Science, 337, 1511

Paardekooper S.-J., Mellema G., 2006, A&A, 459, L17

Paczyńsky B., Wiita P. J., 1980, A&A, 88, 23

Peters P. C., 1964, Phys. Rev., 136, 1224

Rafikov R. R., 2013, ApJ, 774, 144

Rafikov R. R., 2016, ApJ, 827, 111

Ragusa E., Lodato G., Price D. J., 2016, MNRAS, 460, 1243

Roedig C., Sesana A., Dotti M., Cuadra J., Amaro-Seoane P., Haardt F., 2012, A&A, 545, A127

Ryan G., MacFadyen A., 2017, ApJ, 835, 199

Sesana A., Haardt F., Madau P., Volonteri M., 2005, ApJ, 623, 23

Sesana A., Roedig C., Reynolds M. T., Dotti M., 2012, MNRAS, 420, 860

Shakura N. I., Sunyaev R. A., 1973, A&A, 24, 337

Shi J.-M., Krolik J. H., Lubow S. H., Hawley J. F., 2012, ApJ, 749, 118

Syer D., Clarke C. J., 1995, MNRAS, 277, 758

Tanaka T., Menou K., Haiman Z., 2012, MNRAS, 420, 705

Volonteri M., Haardt F., Madau P., 2003, ApJ, 582, 559

Ward W. R., 1997, Icarus, 126, 261

This paper has been typeset from a TEX/LATEX file prepared by the author.